Mon. Not. R. Astron. Soc. **296,** 1045–1056 (1998)

On the Galactic disc age–metallicity relation

Giovanni Carraro,[1,2] Yuen Keong Ng[3] and Laura Portinari[1,4]

[1]*Department of Astronomy, University of Padova, Vicolo dell'Osservatorio 5, I-35122 Padova, Italy*
[2]*SISSA–ISAS, Via Beirut 2–4, I-34014 Trieste, Italy*
[3]*Osservatorio Astronomico di Padova, Vicolo dell'Osservatorio 5, I-35122 Padova, Italy*
[4]*Nordita, Blegdamsvej 17, DK-2100 Copenhagen Œ, Denmark*

Accepted 1998 January 20. Received 1998 January 20; in original form 1997 July 23

ABSTRACT

A comparison is made between the age–metallicity relations obtained from four different types of studies: F and G stars in the solar neighbourhood, analysis of open clusters, galactic structure studies with the stellar population synthesis technique and chemical evolution models. Metallicities of open clusters are corrected for the effects of the radial gradient, which we find to be -0.09 dex kpc^{-1} and most likely constant in time. We do not correct for the vertical gradient, because its existence and value are not firmly established.

Stars and clusters trace a similar age–metallicity relation, showing an excess of rather metal-rich objects in the age range 5–9 Gyr. Galactic structure studies tend to give a more metal-poor relation than chemical evolution models. Neither relation explains the presence of old, relatively metal-rich stars and clusters. This might be caused by uncertainties in the ages of the local stars, or pre-enrichment of the disc with material from the bulge, possibly as a result of a merger event in the early phases of the formation of our Galaxy.

Key words: Galaxy: abundances – Galaxy: evolution – Galaxy: fundamental parameters – Galaxy: general – open clusters and associations: general – Galaxy: structure.

1 INTRODUCTION

The age–metallicity relation (AMR) for nearby stars is a record of the progressive chemical enrichment of the star-forming local interstellar medium during the evolution of the Galactic disc, and so provides useful clues about the star formation and chemical evolution history of the local environment. Metallicity is usually identified with the [Fe/H] ratio. Oxygen would actually be a better tracer and 'chronometer' of metal enrichment (Wheeler, Sneden & Truran 1989), because it is the most abundant metal and it is produced on the well-defined and short time-scale of type II supernovae (SNe). In contrast, iron is released by various sources (both type II and type Ia SNe) with rather different time-scales. Anyway, metallicity is generally determined by the [Fe/H] ratio, because the [O/H] ratio is much more difficult to measure in stellar atmospheres.

⋆E-mail: carraro@pd.astro.it (GC); yuen@pd.astro.it (YKN); portinari@pd.astro.it (LP)

In the solar neighbourhood, the metallicity of stars can be studied in high detail (Edvardsson et al. 1993, hereafter Edv93ea), but the results are liable to large errors in the individual determinations of age. Ng & Bertelli (1988, hereafter NB98) demonstrated that the errors in the age are mainly caused by the large uncertainties in individual distances. Distances need to be known to a 5 per cent accuracy to get reliable ages. In this respect, the ages and metallicities of clusters are more reliable, because one is dealing with a group of stars and therefore the result is less susceptible to individual errors.

An AMR can also be obtained from star count studies, based on the population synthesis technique (Bertelli et al. 1995, 1996; Ng et al. 1995, 1996, 1997). In such studies all the stars along the line of sight are considered. The disc is sampled with respect to age and metallicity in layers with specific effective thicknesses. In this way indications are obtained for the chemical evolution of the disc.

The aim of this paper is to compare the AMRs obtained from various methods and to discuss critically the probable causes for the differences found. In Section 2 we start with

a general overview of the various AMRs and improve them when possible. In Section 3 the relations are compared with one other and probable causes for any discrepancy are outlined. The results are finally summarized in Section 4.

2 AGE–METALLICITY RELATION

In this section we describe the AMRs considered for this study. We start with the AMR obtained from stars in the solar neighbourhood. We then consider the AMR obtained from open clusters, by improving the results from Carraro & Chiosi (1994a, hereafter CC94a) with a larger cluster sample. We continue with the description of the AMR obtained from star count analysis based on the stellar population synthesis technique. Finally, we discuss the AMR obtained from chemical evolution models.

2.1 The solar neighbourhood

Twarog (1980) first showed that nearby stars display an AMR, by applying *uvby*-β photometry and Yale isochrones to obtain the metallicity and the age for two wide samples of stars. As individual data points showed a remarkable dispersion, age bins and average metallicity per bin were used to deduce the local AMR. The metallicity turned out to increase sensitively during disc evolution, rapidly from 13 to 5 Gyr ago, and more slowly after this.

Twarog's data were later re-examined by means of different photometric calibrations with the Vandenberg (1983, 1985) isochrones, resulting in discordant AMRs. Carlberg et al. (1985) limited themselves to only one of the two samples from Twarog, hereby excluding around 50 of the lowest metallicity stars. They obtained a relatively high average metallicity for old stars and a shallower slope of the AMR in the early phases, suggesting that the disc evolution started with a high initial metallicity. On the other hand, Meusinger, Reimann & Stecklum (1991) re-examined both samples from Twarog with Vandenberg's isochrones and with a new calibration for the metallicity index and improved model atmospheres. The resulting AMR was closer to the one obtained by Twarog and had a considerable slope toward high ages. This relation is displayed in Fig. 1.

A new estimate of the local AMR, based on a sample of 189 nearby F and G dwarfs, was performed by Edv93ea. The metallicity is derived from the analysis of high-resolution spectra with theoretical LTE model atmospheres. The ages were determined from fits of the photometric data with Vandenberg (1985) isochrones. The resulting binned AMR is in good agreement, within the large dispersion, with that of Meusinger et al. (1991). Fig. 1 shows the averaged, binned AMR (open squares) from Edv93ea together with the individual data points.

The Edv93ea data set was re-analysed by NB98 by means of Bertelli et al. (1994) isochrones, based on the latest opacity tables. Near the main sequence, high-age isochrones are packed closely together and the deduced ages have considerable uncertainties. The situation changes if a star is on the giant branch: its evolution is relatively fast and the uncertainty in the age becomes considerably smaller. For the determination of the ages, NB98 also took into account the uncertainties on the effective temperature, metallicity and distance of each star; the distances of the stars are obtained from the *Hipparcos* (ESA 1997) parallaxes. In this way, reliable ages were obtained for the stars displayed with large symbols in Fig. 2. The resulting AMR has a small, but distinct slope of ~ 0.07 dex Gyr^{-1} when the stars older than 10 Gyr are considered. However, NB98 suspect that the ages for $t > 10$ Gyr might be overestimated (~ 2 Gyr), because of an improper selection of the isochrones for these stars, which are overabundant in α-elements. It is noteworthy that this relation is essentially no different from that obtained when, for the stars with reliable ages, the ages from Edv93ea are adopted; we refer to NB98 for additional details.

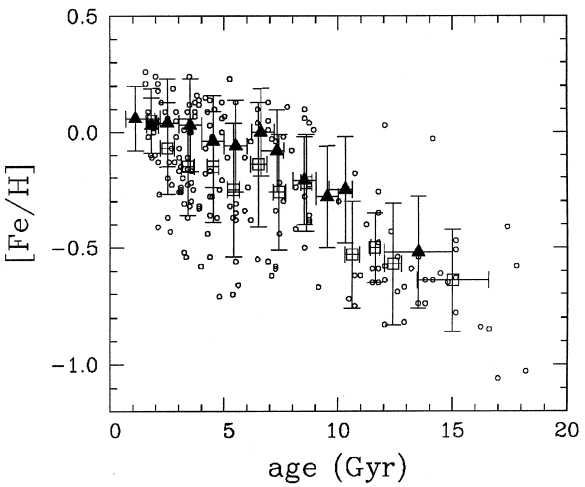

Figure 1. AMR for nearby stars by Meusinger et al. (1991, triangles) and Edvardsson et al. (1993, open squares and open circles).

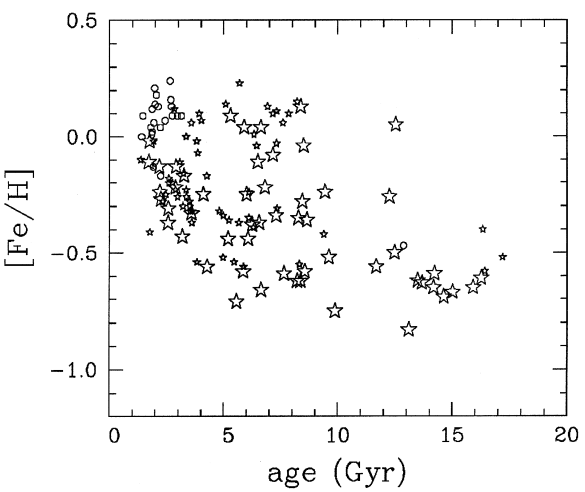

Figure 2. The AMR for nearby stars by Ng & Bertelli (1997). The ages are computed with the distances obtained from the *Hipparcos* parallaxes (ESA 1997). The open circles indicate stars on or near the main sequence with an uncertainty in the age of less than 12 per cent. Open stars are used for giant branch stars. The uncertainty in the age is less than 12 per cent for the large symbols and greater than 12 per cent for the small symbols.

However, the most striking feature of the results mentioned above is the huge scatter around the average trend, which makes the correlation between age and metallicity rather weak, especially for stars with $t < 10$ Gyr. Such a spread in the data must be in part intrinsic, and many possible causes have been suggested: orbital diffusion of stars coupled with radial metallicity gradients, local inhomogeneities in the star-forming gas, inhomogeneous accretion in infalling external gas and overlapping of different galactic substructures, each with its own specific AMR. All the above-mentioned effects may actually contribute to produce the observed scatter, and the new challenge for chemical models is to explain such a large spread in the local AMR (see Section 2.4).

2.2 Open clusters

2.2.1 Sample

Most of the open clusters considered in this paper (Table 1) are taken from the compilation presented by CC94a. We selected from that sample all the clusters for which a homogeneous metallicity determination was available: all the metallicities in Table 1 are in fact obtained spectroscopically and they are in the Boston scale (Friel & Janes 1993; Friel 1995). Therefore, with respect to CC94a we do not consider here NGC 6603, IC 1311, NGC 77804, King 2 and AM 2, because for these clusters the lack of a homogeneous metallicity estimate prevents us from obtaining their age with the same method as for all the other clusters. In addition, the CC94a sample has been updated, including here Berkeley 17 (Kaluzny 1994), Berkeley 20, Berkeley 31, King 5 (Phelps, Janes & Montgomery 1994), Collinder 261 (Mazur, Krzeminski & Kaluzny 1995) and NGC 1245 (Carraro & Patat 1994). Table 1 lists our updated compilation for 37 clusters.

In CC94a, the ages of 10 clusters were determined with stellar isochrones using the synthetic colour–magnitude diagram (CMD) technique (Chiosi et al. 1989). This sample defined a relation between age and ΔV (cf. Cannon 1970; Barbaro & Pigatto 1984; Anthony-Twarog & Twarog 1985; Cameron 1985). The ages of the remaining clusters were obtained through interpolation of this relation; only in a few cases was an extrapolation applied. von Hippel, Gilmore & Jones (1995) noticed for one cluster a discrepancy between the extrapolated ΔV age and the age determined from the white dwarf cooling sequence. This, however, does not imply, as concluded by von Hippel et al., that the isochrone ages are in error. It mainly demonstrates that one has to be cautious with extrapolations.

In this paper, the ages for all the clusters in Table 1 have been determined by fits with the Bertelli et al. (1994) isochrones using the synthetic CMD technique, following the procedure described by Carraro & Chiosi (1994a, 1995). We found for Berkeley 17 and Collinder 261 a different age compared with recent studies (Phelps 1997 and Gozzoli et al. 1996 respectively). In the case of Berkeley 17 the different value can be ascribed to the use of different data sets and different techniques (simple isochrone fitting against synthetic CMDs). The same partly holds for Collinder 261. We use a different data set and a slightly different method. Gozzoli et al. (1996) derived the age from evolutionary

Table 1. Sample of 37 clusters with ages determined by the synthetic CMD technique (2nd column), spectroscopic metallicities in the Boston scale (Friel & Janes 1993; Friel 1995; 3rd column) and corresponding errors (4th column), height above the Galactic plane (5th column) and galactocentric distance (6th column).

Cluster	age(Gyr)	[Fe/H]	r.m.s.	z (pc)	R (kpc)†
Berkeley 17	9.00	−0.29	0.13	170	11.2
Berkeley 19	3.80	−0.50	0.10	300	13.3
Berkeley 20	3.00	−0.75	0.21	2100	16.0
Berkeley 21	3.10	−0.97	0.10	260	14.5
Berkeley 31	4.00	−0.50	0.16	430	12.7
Berkeley 32	3.00	−0.58	0.10	300	12.0
Berkeley 39	6.50	−0.31	0.08	705	11.7
Cr 261	7.00	−0.14	0.14	420	7.6
IC 166	0.85	−0.32	0.20	10	10.7
IC 4651	1.60	−0.16	0.05	100	7.8
King 5	0.80	−0.38	0.20	180	10.5
King 11	6.00	−0.36	0.14	460	10.5
M 67	4.80	−0.09	0.07	415	9.1
Melotte 66	5.46	−0.51	0.11	710	9.4
NGC 188	7.50	−0.05	0.11	570	9.3
NGC 752	1.50	−0.16	0.05	145	8.7
NGC 1193	5.00	−0.50	0.18	1020	12.7
NGC 1245	0.80	+0.14	0.10	460	11.1
NGC 1817	0.80	−0.39	0.04	410	10.3
NGC 2141	2.50	−0.39	0.11	430	12.6
NGC 2158	1.42	−0.23	0.07	95	11.6
NGC 2204	1.74	−0.58	0.10	1200	11.8
NGC 2243	4.50	−0.56	0.17	1260	11.1
NGC 2420	2.10	−0.42	0.07	655	10.3
NGC 2477	0.60	−0.05	0.11	135	9.0
NGC 2506	1.90	−0.52	0.07	460	10.4
NGC 2660	0.70	+0.06	0.10	152	9.2
NGC 3680	1.80	−0.16	0.05	230	8.3
NGC 3960	0.60	−0.34	0.08	180	8.0
NGC 5822	0.45	−0.21	0.12	45	7.9
NGC 6791	8.00	+0.19	0.19	1010	8.4
NGC 6819	2.05	+0.05	0.11	310	8.2
NGC 6939	1.40	−0.11	0.10	255	8.7
NGC 6940	0.60	+0.04	0.10	100	8.3
NGC 7142	4.90	0.00	0.06	495	9.7
NGC 7789	1.35	−0.26	0.06	165	9.4
Tombaugh 2	1.75	−0.70	0.18	1030	15.6

†R is computed with $R_{\odot} = 8.5$ kpc for the distance of the Sun to the Galactic Centre for consistency with previous work.

tracks (Fagotto et al. 1994), while we determined the age from suitably interpolated isochrones (Bertelli et al. 1994). Finally, we performed simulations with synthetic CMDs and used the capability of our code to interpolate between isochrones of different metallicities, adopting for the simulations a metallicity Z corresponding to the observational [Fe/H].

The main advantage of this compilation is the homogeneity of the sample: ages, metallicities and positions in the Galactic disc are all obtained in the same fashion. This homogeneity is not guaranteed when using larger samples as in Friel (1995), Piatti, Claria & Abadi (1995, hereafter P95ea) or Twarog, Ashman & Anthony-Twarog (1997). In addition, completeness is a crucial ingredient in order to explore possible relations between the cluster properties and their position in the Galactic disc. However, it is not possible to gather a complete sample for the old, open clusters in the Galactic disc because of strong selection effects, mainly related to the past dynamical history of the Galactic disc. Many old clusters have probably been disrupted (van den Bergh & McClure 1980; Friel 1995). Taking this limitation into account, we used a statistical approach to find correlations between the fundamental parameters of the clusters, i.e. age, metal abundance and position inside the Galactic disc.

2.2.2 *Multivariate analysis*

The search for correlations has been realized by means of multivariate data analysis (Murtagh & Heck 1987) with the SPSS package (Nie et al. 19075). In particular, we performed the so-called Principal Component Analysis (PCA), which is designed to find a number of independent parameters characterizing multivariate data. This technique is widely used in astronomy; for applications to other astronomical problems we refer to Murtagh & Heck.

The crux of the method is to search for suitable linear coordinate transformations, which are by definition orthogonal, and to diagonalize the covariance matrix from an original set of variables $(x_1, x_2, \ldots, x_n)$ to a new set of variables $(\psi_1, \psi_2, \ldots, \psi_n)$ with a zero mean value:

$$\psi_i = \sum_{k=1}^{n} l_{ik} x_k, \qquad (1)$$

such that the eigenvalues λ_i of the matrix $\langle \psi_i \psi_j \rangle$ are the variances of the data in the direction of the principal component. The corresponding eigenvectors are then used to build new linear combinations from the initial parameters. By convention, the first principal component corresponds to the largest eigenvalue. As a consequence, the first principal component is a minimum-distance fit to a line in the space of the original parameters. The same holds for possible second, third, and so on, principal components.

2.2.3 *Principal components*

In our case the original space of parameters is four-dimensional. The parameters are the age, the metallicity, the z-coordinate and the radial distance R from the Galactic centre (R is computed with $R_\odot = 8.5$ kpc, where $R_\odot$ is the distance of the Sun to the Galactic centre). The straight application of PCA leads to the identification of the two principal components shown in Table 2.

The first principal component ψ_1 gathers more than 50 per cent of the variance. Its coefficients are an indication of the degree of dependence it has on the original parameters. It appears from the first component that the clusters occupy a three-dimensional subspace inside the four-dimensional parameter space: a kind of strongly elongated cigar the main axis of which is almost parallel to the age axis. The old open clusters in Table 1 therefore form a one-parameter family.

The projections of the first principal component on the six planes are $([\mathrm{Fe/H}] - t_9)$, $(z - t_9)$, $(R - t_9)$, $([\mathrm{Fe/H}] - z)$, $([\mathrm{Fe/H}] - R)$ and $(z - R)$. They correspond approximately to the usual regression fits between these pairs of variables. The results are shown in Fig. 3.

A similar analysis is made for the P95ea data set. To be representative, a cluster sample has to be well distributed in age, metallicity and position. Their sample includes 62 clusters with homogeneous metallicities, derived from DDO photometry. The other parameters are non-homogeneous, because only one metal-poor cluster (NGC 23243) with $z > 1$ kpc above the Galactic plane is included, and in addition they did not consider NGC 6791, an old, metal-rich cluster with $z = 1$ kpc. Moreover, about half of the sample (37 clusters) is younger than 1 Gyr and located at $z = 100$ pc. Therefore, homogeneity in age and position is not necessarily guaranteed in their cluster sample. In the PCA analysis we follow for consistency P95ea and do not consider NGC 6791 and Lo 807. The latter cluster is excluded because it lacks an age estimate. Concerning Ru 46, one has to keep in mind that Carraro & Patat (1995) demonstrated that this is likely not an open cluster. Finally, the orbits calculated by P95ea are based on an out-of-date Galaxy model (see for instance Allen & Santillan 1993) and in addition they did not correct the velocity components for Galactic differential rotation (Carraro & Chiosi 1994b).

The results (ψ_{1p}, ψ_{2p}) of the PCA are shown in Table 2, and the projections of the first component shown in Fig. 4 are in the same six planes as those in Fig. 3. The lower eigenvalue and variance of the first principal component for the P95ea sample with respect to our sample are an indication that their data set is less homogeneous.

2.3 Stellar population synthesis

The stellar population synthesis technique is used to generate synthetic Hertzsprung–Russell diagrams (HRDs) from

Table 2. Principal components (ψ_1, ψ_2) and eigenvalues for the open cluster sample listed in Table 1, together with the values (ψ_{1p}, ψ_{2p}) for the Piatti et al. (1995) sample.

l_{ij}	age	[Fe/H]	z	R	λ	*variance*(%)
ψ_1	0.201	−0.849	0.755	0.914	2.167	54.2
ψ_2	0.938	0.284	0.256	−0.153	1.049	26.2
ψ_{1p}	0.624	−0.890	−0.331	0.782	1.903	47.6
ψ_{2p}	0.619	0.100	0.873	−0.011	1.155	28.9

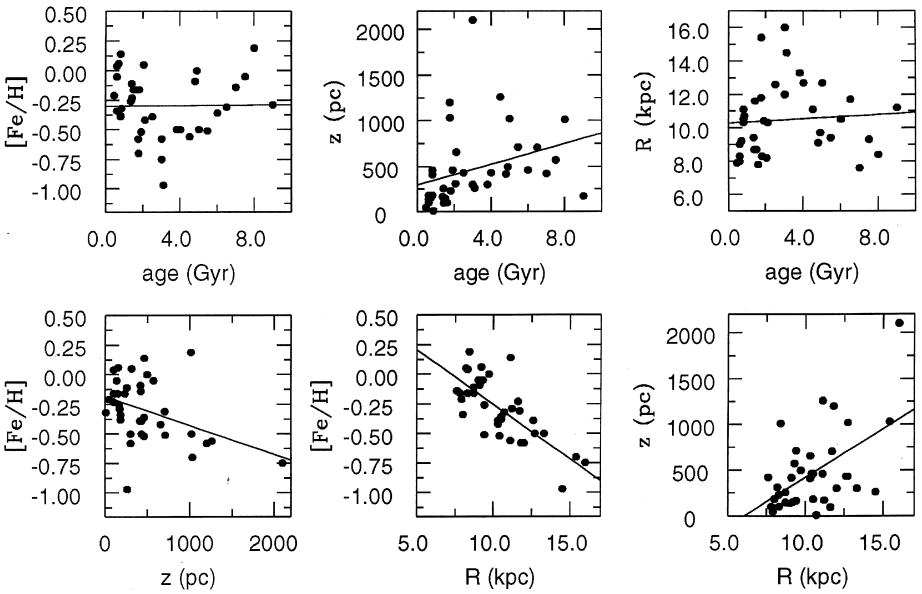

Figure 3. Relation between the fundamental parameters of the open cluster sample given in Table 1, see Sections 2.2.2 and 2.2.3 for details. Solid lines are the projections of the first principal component: $([Fe/H]-t_9)$, $(z-t_9)$, $(R-t_9)$, $([Fe/H]-z)$, $([Fe/H]-R)$ and $(z-R)$.

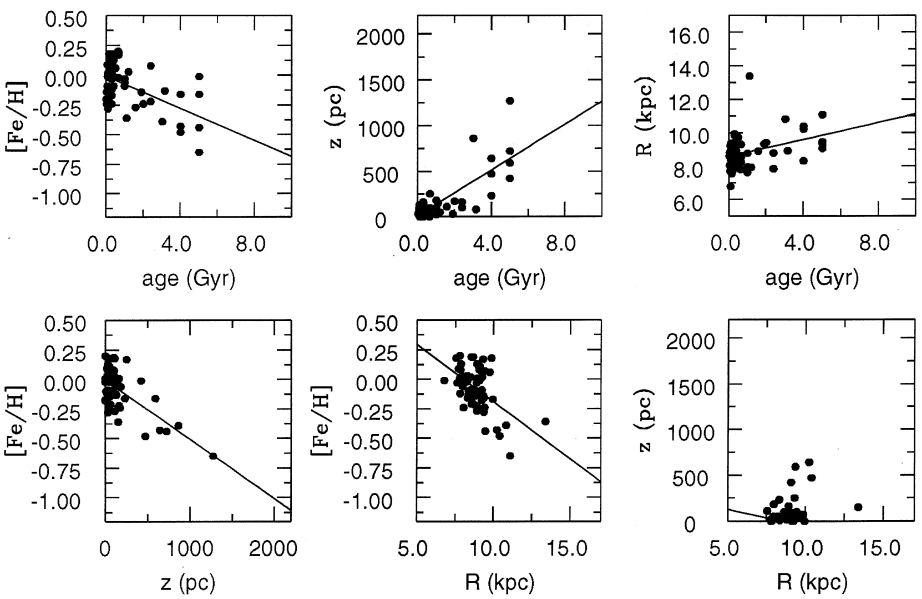

Figure 4. Relation between the fundamental parameters of the sample of open clusters from Piatti et al. (1995), see Sections 2.2.2 and 2.2.3. Solid lines are the projections of the first principal component: $([Fe/H]-t_9)$, $(z-t_9)$, $(R-t_9)$, $([Fe/H]-z)$, $([Fe/H]-R)$ and $(z-R)$.

either stellar evolutionary tracks or isochrones. It is a powerful tool to study resolved stellar populations. The evolutionary phases of a star are linked to each other through libraries of stellar evolutionary tracks. The ratio of the number of stars between different phases is directly related to the relative evolutionary time-scale. This technique has been applied mainly to the analysis of stellar aggregates (Aparicio et al. 1990; Tosi et al. 1991; Vallenari et al. 1992; Carraro et al. 1993; Aparicio & Gallart 1995).

The so-called HRD galactic software telescope (HRD-GST) has been developed to study the stellar populations in our Galaxy (Ng 1994; Ng et al. 1995). The basis is formed by the latest evolutonary tracks calculated by the Padova group (Bertelli et al. 1994 and references cited therein). A smooth metallicity coverage is obtained through interpolation between the sets of tracks from low ($Z=0.0004$) to high ($Z=0.10$) metallicity. Fig. 5 shows a schematic diagram of the HRD-GST; see Ng (1994) and Ng et al. (1995) for additional details.

Synthetic CMDs are generated with a galactic model and ought to be comparable with those obtained from observations. The distribution of the stars along the line of sight is a complex mixture of populations. The ages, metallicities and spatial distributions of the stars from different popula-

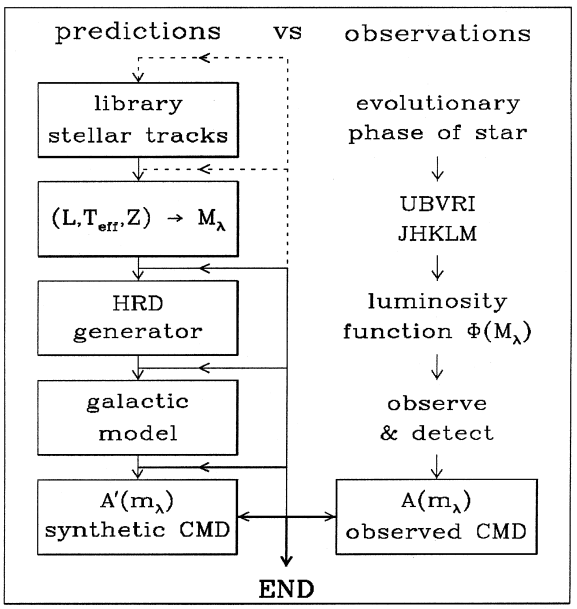

Figure 5. Schematic diagram of the HRD-GST. Input for the stellar population synthesis engine is the Padova library of stellar evolutionary tracks. The luminosities and effective temperatures for each synthetic star of arbitrary metallicity are then transformed to an absolute magnitude in a photometric passband with the method outlined by Bressan, Chiosi & Fagotto (1994) and Charlot, Worthey & Bressan (1996). A synthetic HRD is generated, after specification of the stellar luminosity function through the initial mass function, the star-formation rate and the age and metallicity range. Synthetic stars from those diagrams are then 'observed' and 'detected' with the galactic model, through a Monte-Carlo technique. In this model the density distribution of each galactic component along the line of sight is specified. This results in a synthetic CMD of the field of interest. The synthetic CMD ought to be comparable with the observed CMD, when a realistic set of input parameters is used. If there is a marginal agreement then one should check the input for each step of the HRD-GST.

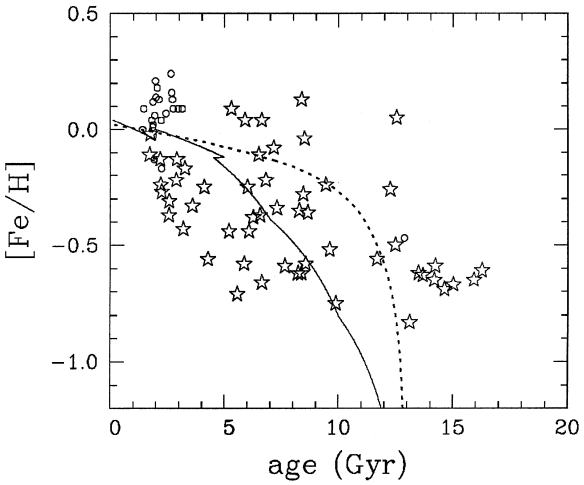

Figure 6. The AMR for stars in the solar neighbourhood (open stars and circles, Ng & Bertelli 1997); see also Fig. 2 for details about the symbol size and uncertainty in the age for these stars; the solid line is the relation obtained for the Galactic disc from studies with the HRD-GST (Ng et al. 1996, 1997); the dotted line is the prediction from the chemical evolution model from Portinari et al. (1998), with an adopted age for the disc of 13 Gyr.

tions contain a wealth of information about the structure, formation and evolution of our Galaxy.

The primary goal of the HRD-GST is to determine the interstellar extinction along the line of sight and to obtain constraints on the galactic structure and age–metallicity relation of the different stellar populations distinguished in our Galaxy. The results obtained thus far have been reported in various papers (Bertelli et al. 1995, 1996; Ng et al. 1995, 1996, 1997). The disc is described by a mixture of subpopulations, each with its specific scaleheight and metallicity, respectively increasing and decreasing with age. The star formation of metal-poor stars in the Galactic disc commenced around 16–13 Gyr ago (Ng 1994; Ng et al. 1997). We adopted 13 Gyr for this paper. Fig. 6 shows the AMR obtained with the HRD-GST together with data from stars in the solar neighbourhood and the line predicted by a chemical evolution model.

2.4 Chemical evolution models

The AMR for nearby stars is a standard constraint for modelling the chemical evolution of the solar neighbourhood, because it is a trace of the progressive storage of heavy elements in the star-forming local interstellar medium.

Most numerical or analytical chemical evolution models for the solar neighbourhood and for the Galactic disc (Matteucci & François 1989; Tosi 1988; Ferrini et al. 1992, 1994; Prantzos & Aubert 1995; Pagel & Tautvaisiene 1995; Timmes, Woosley & Weaver 1995; Chiappini, Matteucci & Gratton 1997; Portinari, Chiosi & Bressan 1998; and references cited in those papers) follow the evolution of chemical abundances for a mixture of stars and gas, which is assumed to be chemically homogeneous in space. The disc is divided into concentric rings, each of which is treated as a homogeneous region. Therefore, such models are aimed at reproducing average features.

Many physical inputs of chemical models are rather poorly known and assumptions need to be made about the star-formation rate (SFR), initial mass function (IMF), infall time-scale, and so forth. These quantities are usually parametrized and then calibrated on observational constraints. The predicted AMR for the solar neighbourhood is sensitive to the adopted SFR, infall time-scale and IMF. All chemical models are basically able to reproduce the observed average AMR (see, for instance, Fig. 8). As already mentioned in Section 2.1, recent studies of the AMR indicate the presence of a significant scatter with respect to the average trend. The scatter in metallicity for a given age is comparable to the overall average increase of metallicity from the early phases of disc evolution to the present time (Edv93ea). As a result, the average AMR no longer represents a tight constraint for chemical evolution models; the new challenge lies now in reproducing the dispersion of the data, rather than the average correlation. More complex chemical models are therefore required, which should include mechanisms inducing the observed

scatter. We briefly summarize here various mechanisms that have been suggested.

(i) *Diffusion of stellar orbits* allows stars to move away from their birthplaces because of scattering of molecular clouds, density waves in the disc or infalling satellite galaxies. This phenomenon is revealed by the observed relation between the age and the velocity dispersion of disc stars (Wielen 1977; Wielen et al. 1992). Diffusion of stars from different birthplaces into nearby orbits results in a spread of metallicities with respect to the expected 'local' metallicity for a given age; François & Matteucci (1993) discuss this effect in the framework of chemical evolution models. Edv93ea derived accurate kinematical data and explored the influence of stellar orbits on the scatter in the AMR; the scatter remains large, even for subsamples with similar orbital properties. This might be an indication that another mechanism is required to explain the scatter, but the argument is still controversial (see Wielen et al. 1996).

(ii) *Non-instantaneous mixing* of stellar nucleosynthesis products in the surrounding gas allows for self-enrichment in molecular clouds and for local inhomogeneities (Malinie et al. 1993). Pilyugin & Edmunds (1996) and van den Hoek & de Jong (1997) combined self-enrichment caused by sequential star formation with episodic infall of relatively metal-poor gas, triggering star formation on time-scales shorter than the time that mixing takes to smear out chemical inhomogeneities. Both sequential star formation and infall are observed to take place in the solar neighbourhood, but each mechanism in itself turns out to be insufficient to match observational evidence; on the other hand, good agreement is found when both processes are allowed to operate together.

(iii) *Different galactic substructures* (halo, thick disc, thin disc and bulge), each with its own AMR, might overlap in the solar vicinity. Pardi, Ferrini & Matteucci (1994) followed the parallel evolution of a halo, a thick disc and a thin disc with different evolutionary rates, and the resulting mixture of stars shows a scatter in the AMR; however, it is lower than the one observed in the solar neighbourhood. Most of all, this explanation is not appealing, because only a low contribution from the thick disc and halo population is expected in the solar neighbourhood from star count analysis. In fact, the expected ratio of metal-poor disc stars with respect to other disc stars is about 0.9 per cent and the ratio of halo/disc $\simeq 1/1500$ (Ng 1994; Ng et al. 1997), resulting in two metal-poor thick disc stars and no halo stars among the Edv93ea F and G stars. The predicted number of stars explains the deficiency of metal-poor stars in Fig. 6. In addition, the expected absence of halo stars is consistent with the disc kinematics of most of the F and G stars in the sample. The observed scatter should therefore be intrinsic to the disc and not related to the overlap with other galactic components.

Therefore, new chemical models need to include the possibility of a more complex and composite evolution of the galactic disc than usually conceived; this in turn adds new, uncertain parameters in the discussion of the chemical history of the disc. As correctly underlined by van den Hoek (1997) and van den Hoek & de Jong (1997), new observational and theoretical constraints are needed to discern between the different processes.

Apart from the problem related to the scatter in the AMR, all chemical models are able to reproduce the main observational constraints of the solar neighbourhood, in spite of the different parametrization and assumptions. On the contrary, differences appear when extending the study to the whole disc. In particular, different predictions are given about the evoluton of radial abundance gradients with time, although all models are tuned to reproduce the present radial gradients of oxygen and other elements. Tosi (1996) directly compares models from different authors and outlines that in some models the present negative gradient is rapidly established and then remains rather unaltered, in other models it first reaches a steeper value than currently observed and then flattens out, and in yet other models a positive gradient is initially established, which then decreases and eventually turns to negative values. In fact, the temporal behaviour of the gradient basically depends on the competition between metal enrichment by stellar ejecta and dilution by infalling metal-poor gas, i.e. on the SFR/infall ratio, at different galactocentric radii and ages. As both the SFR and the infall rate are poorly known because of the uncertainties in the related physical processes, different assumptions can result in different predictions about the evolution of the gradient, though all the models can reproduce the present situation. An observational determination of the radial gradient at different galactic ages would be a strong constraint in discriminating between different chemical models (see Section 3.1.1).

To explain the scatter in the local AMR and to describe the evolution of the whole disc in a more consistent way, new codes with more realistic input physics are required. A start is made with the chemodynamical models of Steinmetz & Müller (1994), Raiteri, Villata & Navarro (1996), Carraro, Lia & Chiosi (1997) and Samland, Hensler & Theis (1997). Although arbitrary assumptions are still needed about the SFR, such models can follow infall and gas exchanges among different galactic regions self-consistently, reducing the number of free parameters and giving a more physical picture of the formation and evolution of the Galaxy.

3 DISCUSSION

We now continue with a comparison of the AMRs discussed in the previous section. We first deal with the radial and vertical metallicity gradients observed in the disc, then we proceed with a discussion of the various AMRs and eventually suggest some improvements.

3.1 Metallicity gradients

To make a meaningful comparison between AMRs deduced from different samples, they ought to be in or rescaled to the same frame of reference. Positional dependency, caused by locally different chemical evolution histories, should be taken into account. When correcting for this, however, one has to consider that the gradients in different age ranges need not be the same; therefore, stars or clusters with different ages are not necessarily expected to trace the same metallicity gradient.

3.1.1 The radial abundance gradient

The local AMR from Edv93ea, binned with respect to age and radial distance, shows a radial dependence of [Fe/H] after a correction of the radial distance for orbital diffusion. The radial gradient seems to be shallower or absent for the oldest stars, but, within the uncertainties inherent in the correction for orbital diffusion and the large scatter in the AMR, the data might also be consistent with a gredient independent of age.

A radial metallicity gradient for open clusters was first found by Janes (1979) and then confirmed by CC94a and Friel (1995). Open clusters are a much better tracer of the radial gradient than nearby stars, both because they span a larger range of galactocentric distances and because they are not affected significantly by orbital diffusion. Indeed, orbit calculations have shown that open clusters do not move far away from their birthplaces (Carraro & Chiosi 1994b). A radial gradient is also traced by H II regions, B stars, planetary nebulae (PNe) and so forth.

B stars and H II regions, because of their short lifetimes, are tracers of the present-day radial gradient (of oxygen abundance). These two different populations seemed to lead to controversial results: the gradient traced by B stars was much shallower (even flat) than the gradient traced by H II regions (see Prantzos & Aubert 1995 and references therein). However, the latest spectroscopic studies for large homogeneous samples of B stars indicate a radial gradient $\mathrm{d[O/H]}/\mathrm{d}R = -0.07$ dex kpc^{-1} (Smartt & Rolleston 1997), in agreement with the gradient deduced from H II regions, so that nowadays the former discrepancy appears to be solved.

As pointed out in Section 2.4, the present radial gradient provides a constraint for chemical evolution models, but to discern between different models one needs to know how the gradient evolved in the past. Open clusters are an ideal template for this analysis, because they have well-determined ages, metallicities and galactocentric distances.

We analyse our homogeneous cluster sample of Table 1. We divide the sample into age bins, and for each bin we derive the gradient by means of a weighted least-squares fit in the [Fe/H] versus R plane (using a version of the code by Pagel & Kazlauskas 1992). In the fitting procedure the weights are the errors on [Fe/H], also listed in Table 1. A similar analysis was performed by Tosi (1995), but with a smaller sample. Our results for the four age-bins, each 2 Gyr in width, are shown in Fig. 7 and the slopes $\mathrm{d[Fe/H]}/\mathrm{d}R$ of the gradient for the different age-binning are listed in Table 3. In panels (b)–(d) the gradient of panel (a) is included for comparison.

Note that for the determination of the radial gradient, neither CC94a nor P95ea considered separate age groups properly. The P95ea data set is basically a young sample ($t < 1$ Gyr), however, their radial gradient of -0.07 dex kpc^{-1} reflects in fact the present day gradient.

Table 3 displays the effects of different age-binning on the derived radial gradients; indicated errors are standard deviations. Before commenting on the outcome, a caveat has to be stressed: the number of objects involved in this analysis is relatively low, so statistically the results are not very significant. They show a trend, which requires verification with a larger sample.

By selecting 2–3 Gyr wide age bins, the results are similar and indicate that the present-day gradient is a little shallower than the past one; the middle epoch seems to display a steepening of the gradient. The choice of wider bins (4 Gyr) basically suggests the same thing: the present-day gradient appears again to be shallower. On the other hand, choosing a bin width of 5 Gyr we obtain a different result, probably because of a mixing of the present- and middle-epoch gradients in the lower age bin. However, in this last case the statistics is much poorer, because we are left with only eight clusters older than 5 Gyr versus 29 in the younger bin.

For the whole sample we derived an average gradient of -0.09 dex kpc^{-1}, see Fig. 7(e); for any age bin in Table 3 the gradient is close to this average value, within the errors. Overall, our sample of clusters seems to show that the radial gradient has not changed much with time, although a hint can be seen for a steeper gradient in the past, at intermediate ages. Therefore, chemical models predicting either a constant gradient or a slightly steeper negative gradient in the past seem to be favoured with respect to models predicting a gradient that settles to the current negative value, starting from positive initial values. For a detailed comparison of various chemical models, we refer to fig. 5 of Tosi (1996) and references quoted therein. Unluckily, because of the large scatter and the small number of clusters in the higher age bins, one cannot actually draw a firm conclusion.

The presence of a metallicity gradient for open clusters has been questioned by Twarog et al. (1997), who find no gradient for the clusters in their sample at galactocentric radius below 10 kpc. However, their fig. 3b displays that the majority of these clusters are located between 7.5 and 9.5 kpc and have an overall spread of more than 0.2 dex in metallicity. Over a distance range of only 2 kpc, our average gradient corresponds to a metallicity difference smaller than 0.2 dex. Therefore, within that dispersion our results are not necessarily at odds with their sample. In addition, Twarog et al.'s claim that open clusters display a step function with a discontinuity at 10 kpc rather than a gradient in metallicity should be verified by separating in age groups. The step function could be a consequence of insufficient discrimination between the contributions from different age groups, because the sample inside $R = 10$ kpc is heavily weighted toward clusters younger than 1 Gyr, while the outer clusters are predominantly older.

The radial gradient and its age dependence have been studied also by means of PNe. Maciel & Köppen (1994) find an oxygen gradient the present value of which is in agreement with that of H II regions. It seems that the gradient has remained roughly constant, or perhaps it was slightly shallower in the past. Unlike open clusters, however, PNe have rather uncertain ages and distances, and their present location might have been spoiled by orbital diffusion. All these factors introduce uncertainties in the derived age dependence of the gradient. Considering the indications from nearby stars, open clusters and PNe together, the most sensible assumption is that the gradient remained roughly constant in time.

Star counts with the HRD-GST are not sensitive enough to detect a radial gradient within a single-age population. Indeed, a gradient of -0.21 dex kpc^{-1} is already induced by

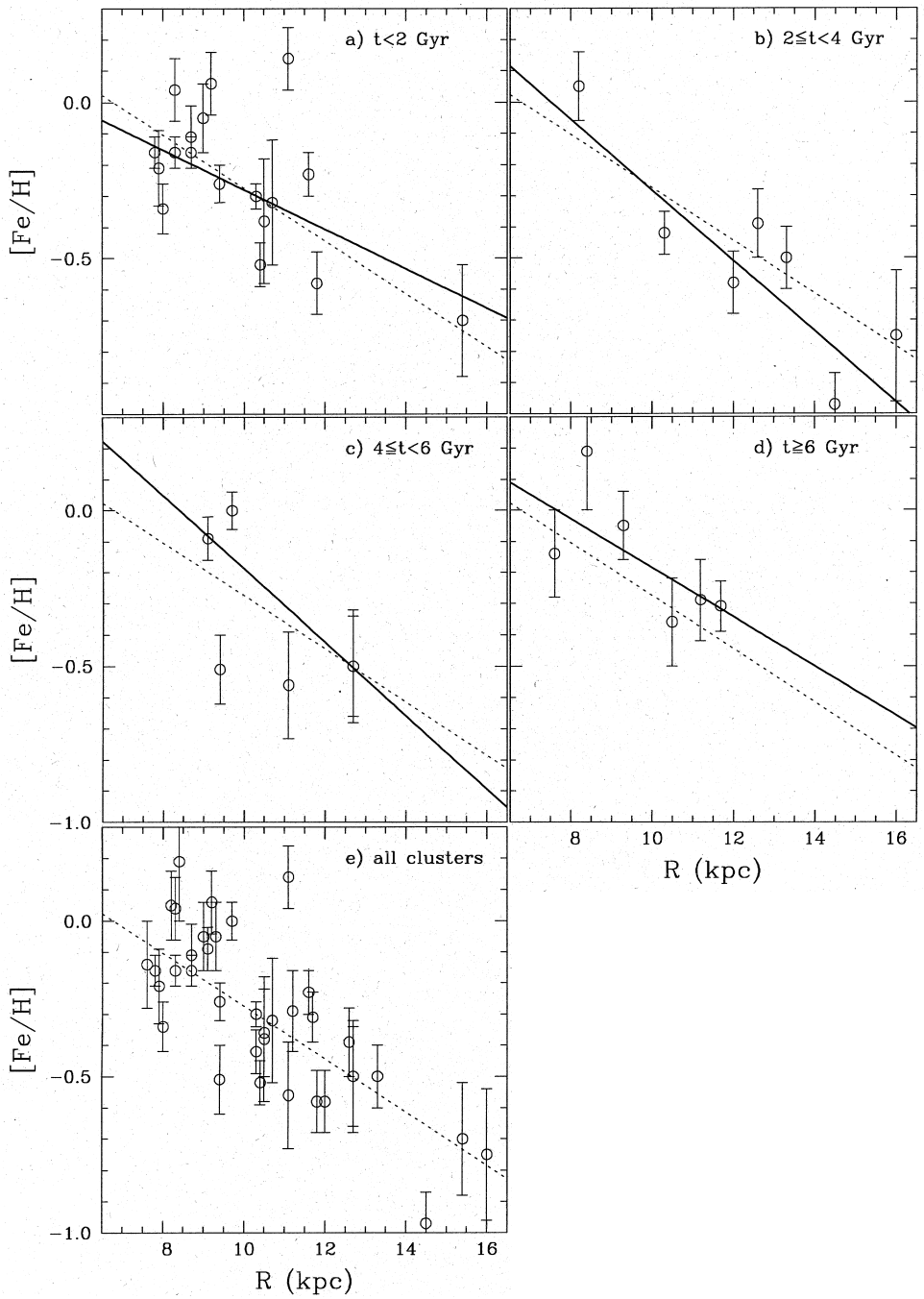

Figure 7. Radial abundance gradients for our sample of open clusters binned in different age ranges. The dashed line (panels a–e) shows the average gradient (-0.09 dex kpc^{-1}) as determined from all the clusters from Table 1. The solid lines in panels a–d show the gradients determined for the corresponding age ranges (-0.06, -0.11, -0.12 and -0.08 dex kpc^{-1}, respectively).

differences in scalelengths among populations of different ages, while within a single-age population the intrinsic gradient of -0.09 dex kpc^{-1} is masked out by the adopted extinction along the line of sight.

3.1.2 The vertical abundance gradient

The existence of a vertical metallicity gradient among old open clusters is controversial. Friel (1995) and CC94a do not find evidence for such a gradient, whereas P95ea do find a correlation between [Fe/H] and vertical position. By binning the data in z they obtained a gradient equal to -0.34 dex kpc^{-1}. Their sample contains only one cluster above 1 kpc, together with four clusters above 500 pc. In addition they did not consider NGC 6791, which is high above the plane (1 kpc) and metal-rich. From our sample the resulting slope is shallower: -0.25 dex kpc^{-1}, not strongly dependent on any particular cluster (Fig. 3, bottom left panel).

However, a caveat is to be stressed, because to estimate the vertical gradient one should disentangle the effects of vertical, radial and age dependence. In principle, one

Table 3. Radial gradient with different age binning.

Age bin (Gyr)	Bin population	$\frac{d[Fe/H]}{dR}$ (dex/kpc)
$t<2$	18	-0.064 ± 0.013
$2\leq t<4$	7	-0.113 ± 0.018
$4\leq t<6$	6	-0.118 ± 0.026
$t\geq6$	6	-0.079 ± 0.033
$t<3$	21	-0.068 ± 0.012
$3\leq t<6$	10	-0.135 ± 0.016
$t\geq6$	6	-0.079 ± 0.033
$t<4$	25	-0.086 ± 0.009
$t\geq4$	12	-0.096 ± 0.024
$t<5$	29	-0.088 ± 0.009
$t\geq5$	8	-0.061 ± 0.029
global	37	-0.085 ± 0.008

should first bin the sample in homogeneous subsamples with respect to age and galactocentric distance, and only then analyse the vertical trend. Then, however, there are not enough clusters in the bins to constrain the vertical gradient reliably. In addition, open clusters form an incomplete sample because of tidal disruption, which is more effective close to the Galactic mid-plane. Therefore, clusters at low galactic latitudes are preferentially destroyed, which might introduce a bias in the determination of the vertical gradient.

Ng et al. (1996) have demonstrated that both the radial and the vertical distributions of open clusters contain information about the scalelength and scaleheight of the Galactic stellar populations. In the case of field stars, orbital diffusion is expected to be effective enough to smooth out a vertical metallicity gradient within a single-age population, so that the vertical structure of the disc is dominated by the different scaleheights of different age populations. Indeed, in star counts the younger, metal-rich stars are confined to regions close to the Galactic mid-plane, while the older, metal-poorer stars with a larger scaleheight dominate at larger vertical distances from the Galactic plane. As a consequence, in star counts a vertical metallicity gradient is caused by sampling of different age populations rather than reflecting a gradient within a single-age population.

In star counts, radial and vertical abundance gradients are primarily expected because of differences between the scalelength and scaleheight of different stellar age populations. As the relative differences in scalelength are small with respect to those in scaleheight, these latter dominate the HRD-GST star count analysis. A strong vertical abundance gradient in star counts is therefore a hint that insufficient discrimination was made for the different age groups within a data set. A metallicity gradient within an age population is a second-order effect.

Almost all open clusters of a given age are found at distances larger than three times the exponential scalelength and scaleheight for the corresponding stellar populations of the HRD-GST. The vertical gradient resulting from stellar mixes of different ages, computed at the 'transition' region toward open clusters, is -0.40 dex kpc^{-1}. This value is comparable to the one found by P95ea, confirming that their gradient could indeed be caused by insufficient discrimination between different age groups.

The orbits of clusters are less affected by orbital diffusion than those of field stars. Once a vertical gradient for open clusters has been established unambiguously, therefore, it can provide an important clue about the disc formation history. As already stressed, however, current samples do not give conclusive indications.

3.2 The galactic disc AMR

Fig. 6 shows various AMRs, derived from

(i) stars in the solar neighbourhood with the ages from NB98 (open circles and open stars);
(ii) the HRD-GST population synthesis analysis for the Galactic disc from Ng et al. (1996, 1997; solid line);
(iii) a chemical evolution model from Portinari et al. (1998; dotted line).

The disc AMR obtained from the HRD-GST is determined from star counts towards the North Galactic Pole and the Galactic Centre. No correction for radial or vertical gradients is applied, because star counts are not sensitive to gradients within single-age populations, see Sections 3.1.1 and 3.1.2. For $t<5$ Gyr, AMR(HRD-GST: disc) $\simeq$ AMR(chemics). Between $t=5$ and 13 Gyr the metallicity of AMR(chemics) is higher than that of AMR(HRD-GST: disc). Indeed, star counts tend to follow the metal-poorer trend, which is more populated and therefore has a larger weight.

Using open clusters to trace the AMR has the main advantage that cluster ages are much more reliably determined than the ages of single field stars, but also the additional problem of the radial and/or vertical dependence of cluster metallicity. Cameron (1985) was the first to derive an AMR from open clusters after correcting for the radial gradient, with the aim of cleaning the data from the space dependence. A unique radial correction should not be applied recklessly to different age groups, however, because of the possible age dependence of the radial gradient (Section 3.1.1). Unluckily, the age dependence of the radial gradient is poorly constrained and any confident correction for the radial gradient of open clusters is spoiled. Our sample is consistent with a radial gradient that is constant in time; therefore we derive from it the AMR shown in Fig. 8 by correcting for a gradient of -0.09 dex kpc^{-1}, independent of age. Still, one should bear in mind this uncertainty in the correction when comparing the AMR of open clusters with the local AMR of nearby stars. In addition, we did not apply any correction for the vertical gradient, because its value and even its existence are not yet clearly established. Fig. 8 shows that the AMRs of open clusters and stars are in good agreement, both showing a similar trend in the scatter. We also notice that both relations show a lack of scattered points on the metal-rich side in the age range 3–5 Gyr and/or an excess of relatively metal-rich objects in the range 5–9 Gyr.

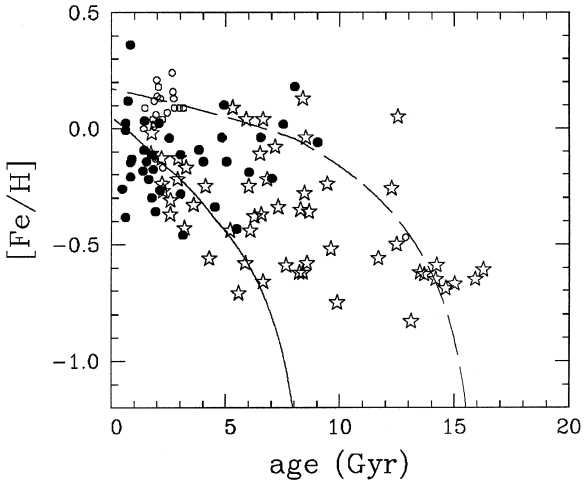

Figure 8. The AMR for open clusters from Table 1 (filled dots) versus the solar neighbourhood one. The metallicities of the open clusters are corrected according to the global radial gradient: $[Fe/H]_{corr} = [Fe/H]_{mean} - 0.09(R_{\odot} - R)$ (kpc). Included in this figure is a suggested improvement for the description of the AMR with two separate components for the HRD-GST. The adopted age for the start of the formation of the 'young' disc component (solid line) is 8.5 Gyr and 16 Gyr for the 'old' disc component (long-dashed line).

3.3 The role of the bulge/bar

The upturn of the metallicity of the open clusters, possibly with a peak near $t \simeq 8$ Gyr, might be related to the formation of the triaxial bar structure. Ng et al. (1996) obtained a comparable age and metallicity range ($t = 8$–9 Gyr, $Z = 0.005$–0.030) for this structure. The bar, however, does not explain the presence of metal-rich stars in the solar neighbourhood, because its local density with respect to local disc stars is too low. In addition, some of the metal-rich stars are older than the bar.

At $t \simeq 8$ Gyr, the stars in the solar neighbourhood are metal-richer than expected from the AMR(HRD-GST: disc) and AMR(chemics). The calculations from Samland et al. (1997) suggest that this could be caused by pre-enrichment with material originating from type II SNe from the bulge. On the other hand, if the 'bar' structure formed through a merger event some of the metal-rich stars from the inner disc or bulge regions could have migrated near to the solar neighbourhood and settled down there. This could explain the presence of rather metal-rich clusters and stars between 5 and 9 Gyr. Suitable dynamical models are however, required (Mihos & Hernquist 1996) to explore and check the merger/capture scenario properly against all the observational constraints.

3.4 Improvements

The comparison of the AMRs from various methods suggests some improvements.

(i) *The solar neighbourhood:* a new sample of stars with spectroscopic metallicities and reliable ages is desirable and better ages are needed for $t > 10$ Gyr.

(ii) *Open and globular clusters:* the sample of open clusters should be enlarged to verify the lack of relatively metal-rich objects in the age range 3–5 Gyr, because the apparent 'U-shape' of the AMR might provide clues about infalling and/or merger events. The old, metal-rich open clusters and the young, metal-rich globular clusters could indicate when the transition between the two types of clusters actually occurred and provide a clue as to whether this could be initiated by the formation of the Galactic bar. The high galactic foreground and background contamination in the colour–magnitude diagrams of the metal-rich globular clusters suggests a combined approach with a galactic population model, to obtain a self-consistent interpretation about the age, metallicity, distance and extinction towards the clusters.

(iii) *Stellar population synthesis:* a second, old and metal-rich disc component should be included in the HRD-GST description of the disc (see Fig. 8) and its nature should be investigated.

(iv) *Chemical evolution models:* possible pre-enrichment and/or influence of the bulge and bar should be considered to explain the metal-rich part of the AMR at high ages. Chemodynamical models look promising in this respect. In particular, with the Lagrangian approach (Raiteri et al. 1996; Carraro et al. 1997), the behaviour of the gas settling down in the disc, vertical and radial infall, outflows and so on can be followed. In addition, such models are suitable for studying merging and capture events.

4 CONCLUSIONS

We compared the Galactic disc AMRs obtained from four different points of view. Our results are briefly outlined here.

(i) For the first time a multivariate analysis of a large, homogeneous sample of open clusters was performed, and the correlations between cluster parameters were unravelled with an a priori approach.

(ii) We investigated the radial gradient and its time evolution, although a larger sample of open clusters would be required to constrain the past behaviour of the gradient better.

(iii) We showed that an apparent strong vertical gradient in open clusters is likely caused by insufficient discrimination betweeen different age groups.

(iv) Considering our improved sample of open clusters and a subsample of local stars with reliable ages, both sets of objects trace a similar AMR, the peculiar shape of which in the range 3–9 Gyr ago might give clues about past infall or merger events.

ACKNOWLEDGMENTS

GC thanks Professor E. Cappellaro for kind assistance in using SPSS. G. Bertelli is acknowledged for valuable suggestions and discussions. We also thank the anonymous referee for constructive suggestions. This research is supported by the TMR grant ERBFMRX-CT96-0086 from the European Community (Network: Formation and Evolution of Galaxies), by the Italian Ministry of University, Scientific Research and Technology (MURST) and by the Italian

Space Agency (ASI). LP also acknowledges financial support from the Danish Rektorkollegiet.

REFERENCES

Allen C., Santillan A., 1993, Rev. Mex. Astron. Astrofis., 25, 39
Anthony-Twarog B. J., Twarog B. A., 1985, ApJ, 291, 595
Aparicio A., Gallart C., 1995, AJ, 110, 2105
Aparicio A., Bertelli G., Chiosi C., Garcia-Pelayo J. M., 1990, A&A, 240, 262
Barbaro G., Pigatto L., 1984, A&A, 136, 355
Bertelli G., Bressan A., Chiosi C., Fagotto F., Nasi E., 1994, A&AS, 106, 275
Bertelli G., Bressan A., Chiosi C., Ng Y. K., Ortolani S., 1995, A&A, 301, 381
Bertelli G., Bressan A., Chiosi C., Ng Y. K., 1996, A&A, 310, 115
Bressan A., Chiosi C., Fagotto F., 1994, ApJS, 94, 63
Cameron L. M., 1985, A&A, 147, 47
Cannon R. D., 1970, MNRAS, 150, 111
Carlberg R. G., Dawson P. C., Hsu T., Vandenberg D. A., 1985, ApJ, 294, 674
Carraro G., Chiosi C., 1994a, A&A, 287, 761 (CC94a)
Carraro G., Chiosi C., 1994b, A&A, 288, 751
Carraro G., Chiosi C., 1995, in Alfaro, E. J., Delgado A. J., eds, The formation of the Milky Way. Cambridge Univ. Press, Cambridge, p. 175
Carraro G., Patat F., 1994, A&A, 289, 297
Carraro G., Patat F., 1995, MNRAS, 276, 563
Carraro G., Bertelli G., Bressan A., Chiosi C., 1993, A&AS, 101, 381
Carraro G., Lia C., Chiosi C., 1998, MNRAS, in press
Charlot S., Worthey G., Bressan A., 1996, ApJ, 457, 625
Chiappini C., Matteucci F., Gratton R., 1997, ApJ, 477, 765
Chiosi C., Bertelli G., Meylan G., Ortolani S., 1989, A&A, 219, 167
Edvardsson B., Andersen J., Gustafsson B., Lambert D. L., Nissen P. E., Tomkin J., 1993, A&A, 275, 101 (Edv93ea)
ESA, 1997, The *Hipparcos* and *Tycho* Catalogue, ESA SP-1200
Fagotto F., Bressan A., Bertelli G., Chiosi C., 1994, A&AS, 104, 365
Ferrini F., Matteucci F., Pardi M. C., Penco U., 1992, ApJ, 387, 138
Ferrini F., Molla M., Pardi M. C., Diaz A. I., 1994, ApJ, 427, 745
Friel E. D., 1995, ARA&A, 33, 381
Friel E. D., Janes K. A., 1993, in ASP Conf. Ser. Vol. 13, The Formation and Evolution of Star Clusters. Astron. Soc. Pac., San Francisco, p. 569
François P., Matteucci F., 1993, A&A, 280
Gozzoli E., Tosi M., Marconi G., Bragaglia A., 1996, MNRAS, 283, 66
Janes K. A., 1979, ApJS, 39, 135
Kaluzny J., 1994, Acta Astron., 44, 247
Maciel W., Köppen J., 1994, A&A, 282, 436
Malinie G., Hartmann D. H., Clayton D. D., Mathews G. J., 1993, ApJ, 413, 633
Matteucci F., François P., 1989, MNRAS, 239, 885
Mazur B., Krzeminski W., Kaluzny J., 1995, MNRAS, 273, 59
Meusinger H., Reimann H. G., Stecklum B.l, 1991, A&A, 245, 57
Mihos J. C., Hernquist L., 1996, ApJ, 464, 641
Murtagh F., Heck A., 1987, Multivariate Data Analysis. Astrophysics and Space Science Library
Ng Y. K., 1994, PhD thesis, Leiden Univ.
Ng Y. K., Bertelli G., 1998, A&A, 329, 343 (NB98)
Ng Y. K., Bertelli G., Bressan A., Chiosi C., Lub J., 1995, A&A, 295, 655 (Erratum: A&A, 301, 318)
Ng Y. K., Bertelli G., Chiosi C., Bressan A., 1996, A&A, 310, 771
Ng Y. K., Bertelli G., Chiosi C., Bressan A., 1997, A&A, 324, 65
Nie N. H., Hadlai Hull C., Jenkins J. G. et al., 1975, SPSS, Statistical Package for the Social Science, 2nd edn. McGraw-Hill, New York
Pagel B. E. J., Kazlauskas A., 1992, MNRAS, 256, 49
Pagel B. E. J., Tautvaisiene G., 1995, MNRAS, 276, 505
Pardi M. C., Ferrini F., Matteucci F., 1994, ApJ, 444, 207
Phelps R. L., 1997, ApJ, 483, 826
Phelps R. L., Janes K. A., Montgomery K. A., 1994, AJ, 107, 1079
Piatti A. E., Claria J. J., Abadi M. G., 1995, AJ, 110, 2813 (P95ea)
Pilyugin L. S., Edmunds M. G., 1996, A&A, 313, 783
Portinari L., Bressan A. G., Chiosi C., 1998, A&A, in press
Prantzos N., Aubert O., 1995, A&A, 302, 69
Raiteri C. M., Villata M., Navarro J. F., 1996, A&A, 315, 105
Samland M., Hensler G., Theis Ch., 1997, ApJ, 476, 544
Smartt S. J., Rolleston W. R. J., 1997, ApJ, 481, L47
Steinmetz M., Müller E., 1994, A&A, 281, L97
Timmes F. X., Woosley S. E., Weaver T. A., 1995, ApJS, 98, 617
Tosi M., 1988, A&A, 197, 33
Tosi M., 1995, in Alfaro E. J., Delgado A. J., eds, The formation of the Milky Way. Cambridge Univ. Press, Cambridge, p. 153
Tosi M., 1996, in Leitherer C., Fritze-von Alvensleben U., Huchra J., eds, ASP Conf. Ser. Vol. 98, From Stars to Galaxies. Astron. Soc. Pac., San Francisco, p. 299
Tosi M., Greggio L., Marconi G., Focardi P., 1991, AJ, 102, 951
Twarog B. A., Ashman K. M., Anthony-Twarog B. J., 1997, AJ, 114, 2556
Vallenari A., Chiosi C., Bertelli G., Meylan G., Ortolani S., 1992, AJ, 104, 1100
Vandenberg D. A., 1983, ApJS, 51, 29
Vandenberg D. A., 1985, ApJS, 58, 711
van den Bergh S., McClure R. D., 1980, A&A, 80, 360
van den Hoek L. B., 1997, PhD thesis, Univ. Amsterdam
van den Hoek L. B., de Jong T., 1997, A&A, 318, 231
von Hippel T., Gilmore G., Jones D. H. P., 1995, MNRAS, 273, L39
Wheeler J. C., Sneden C., Truran J. W., Jr, 1989, ARA&A, 27, 289
Wielen R., 1977, A&A, 60, 263
Wielen R., Dettbarn C., Fuchs B. et al., 1992, IAU Symp. 149, p. 81
Wielen R., Fuchs B., Dettbarn C., 1996, A&A, 314, 438